Supporting Information

Ultra-efficient perfluorooctanoic acid capture enabled by a novel MOF-derived Cu/Zn bimetallic spherical porous carbon

Kunpeng Xue[a,b], Heng Lin[a], Dan Cao[e], Na Ma[c], Wei Dai[a,*], and Limin Zhang[d,*]

[a] *Key Laboratory of the Ministry of Education for Advanced Catalysis Materials, College of Chemistry and Materials Science, Zhejiang Normal University, Jinhua 321004, People's Republic of China*

[b] *One Two Chromatography Technology (Zhejiang) Co., Ltd, Jinhua 321000, People's Republic of China*

[c] *College of Geography and Environmental Sciences, Zhejiang Normal University, Jinhua, 321004, PR China*

[d] *School of Environment, Jiangsu Province Engineering Research Center of Environmental Risk Prevention and Emergency Response Technology, Jiangsu Engineering Lab of Water and Soil Eco-remediation, Nanjing Normal University, No. 1 Wen yuan Road, Nanjing, Jiangsu, 210023 P.R. China*

[e] *unit of Jinhua Customs Comprehensive Technology Service Center, No. 1000, Songlian Road, Jindong District, Jinhua City, Zhejiang Province*

321015

*Heng Lin equally contributed to this work as Kunpeng Xue, and they are both first authors.

2.1. Chemicals and characterization equipment

Copper nitrate trihydrate ($Cu(NO_3)_2 \cdot 3H_2O$, >99.0%), zinc nitrate hexahydrate ($Zn(NO_3)_2 \cdot 6H_2O$, >99.0%), trimesic acid ($C_9H_6O_6$, >99.0%), polyvinylpyrrolidone ($(C_6H_9NO)_n$, >99.0%), glucose ($C_6H_{12}O_6$, >99.0%), N,N-dimethylformamide (C_3H_7NO, >99.0%), ethanol (C_2H_5OH, >99.0%), methanol (CH_3OH, >99.0%), sodium hydroxide (NaOH, >96.0%), hydrochloric acid (HCl, >36.0%), perchloric acid ($HClO_4$, >65.0%), nitric acid (HNO_3, >65.0%), sulfuric acid (H_2SO_4, >65.0%) were purchased from China Pharmaceutical Chemical Reagent Co..

The surface morphology, characteristics, and the synthesized samples' elemental composition were observed using scanning electron microscopy (SEM, GeminiSEM300, DE) and energy-dispersive X-ray spectroscopy (EDS, OXFORD X-Max, UK). The structure and crystal phases of the materials were identified using X-ray diffraction (XRD, D8 Advance, Bruker, DE) within the range of $5° < 2\theta < 80°$. The samples were prepared using the potassium bromide method, and Fourier-transform infrared spectroscopy (FT-IR, Nicolet NEXUS 670, Thermo, U.S.) was employed to analyze the surface functional groups of the adsorbent. Quantitative analysis of N_2 adsorption-desorption data was conducted at 77.15 K using an Autosorb-IQ analyzer (Micromeritics, ASAP2020, U.S.) to assess the pore volume, specific surface area, and pore size distribution of the adsorption material. X-ray photoelectron spectroscopy (XPS) was employed to determine the samples' elemental composition and chemical states (XPS, Escalab 250XI, Thermo, U.S.). The zeta potential of the adsorption

material was measured using a Zetasizer Nano ZS (Malvern, UK), with water as the dispersant. Before measurement, the samples were heated at 373.15 K under vacuum for 12 hours to remove moisture and impurities.

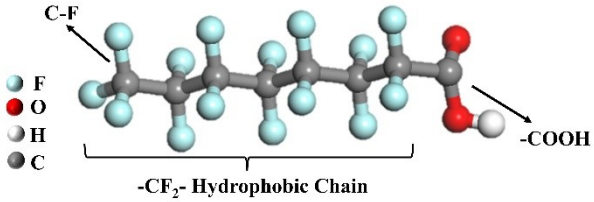

Scheme S1 PFOA stick model diagram.

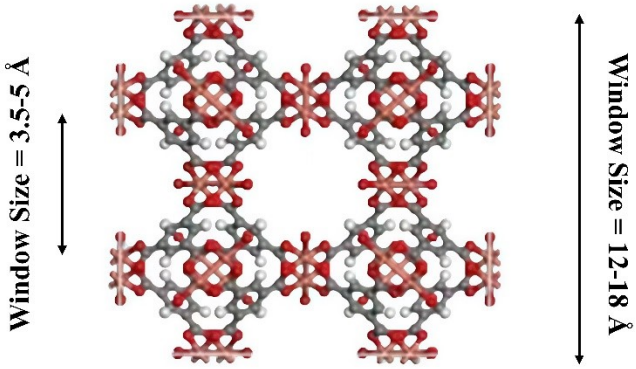

Scheme S2 Perspective view of the topology of SPC (Cu/Zn-BTC).

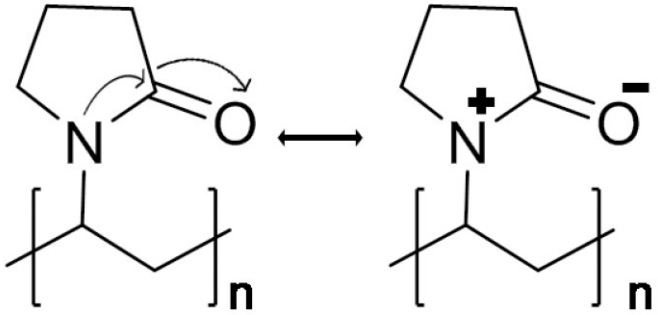

Scheme S3 Resonance structure of PVP.

Table S1 The main properties and structure of perfluorooctanoic acid.

Organic pollutants	Molecular structure	Molecular formula	Molecular dimension	p*K*a
Perfluorooctanoic acid	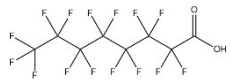	$C_8HF_{15}O_2$	1.05×0.5×0.6 nm	-0.5

Table S2 The high-performance liquid chromatography chart of perfluorooctanoic acid.

Retention period (min)	Area (μV*s)	high degree (μV)	breadth (s)	trailing tail	Theoretical plate number
6.22	263807	37700706	33.00	1.21	18116

Table S3 Structural properties of SPC(5-(Cu/Zn-BTC)) samples.

Sample	S_{BET} (m^2/g)	V_{total} (cm^3/g)	Average pore diameter (nm)
SPC(Cu-BTC)	998	0.42	2.05
SPC(Zn-BTC)	683	0.31	3.62

SPC(5-(Cu/Zn-BTC))	901	0.52	4.02

Table S4 Adsorption isotherm models used in this study and their linear forms.

Isotherm	Nonlinear form	Linear form	Plot
Langmuir	$q_e = \frac{K_L C_e}{1 + K_L C_e}$	$\frac{C_e}{q_e} = \frac{1}{q_L \bullet K_L} + (\frac{1}{q_L}) \bullet C_e$	$\frac{C_e}{q_e}$ versus C_e
Freundlich	$q_e = K_f C_e^{\frac{1}{n}}$	$lnq_e = lnK_f + (\frac{1}{n}) \bullet lnC_e$	lnq_e versus lnC_e
Temkin	$e^{qe} = (K_T C_e)^{\frac{RT}{b_T}}$	$q_e = \frac{RT}{b_T} lnK_T + \frac{RT}{b_T} lnC_e$	q_e versus lnC_e
D-R	$q_e = q_s e^{(-K_D \varepsilon^2)}$	$lnq_e = lnq_s - K_D \varepsilon^2$ $E = \frac{1}{\sqrt{2K_D}}$	lnq_e versus ε^2

Where q_e is the maximum capacity of adsorption in mg/g; K_L is a constant related to the affinity of the binding sites in L/mg; 'K_f' and 'n' are the measures of adsorption capacity and intensity of adsorption; R is the universal gas constant; b_T is related to the heat of adsorption in kJ/mol. T is the absolute temperature in K; R is the universal gas constant; K_T is the Temkin constant about the capacity of adsorption in L/g; q_s is the D-R isotherm constant in mg/g; K_D stands for the constant that is relevant to the adsorption energy in mol^2/kJ^2; ε represents the Polanyi potential constant in kJ/mol.

Table S5 Summary of fitting parameters of the adsorption isotherm model of PFOA by SPC(Cu-BTC) and others.

Samples	Langmuir			Freundlich			Temkin			D-R		
	$C_e/q_e=(1/q_{max})*C_e+1/(K_L*q_{max})$			$\ln q_e=\ln K_f+(1/n)*\ln C_e$			$q_e=RT/b_T*\ln K_T(Ce)$			$lnqe=lnqs-K_D\varepsilon^2$		
	q_m (mg/g)	K_L (L/mg)	R^2	K_f (L/g)	n	R^2	b_T (J/mol)	K_T (L/mg)	R^2	q_s (mg/g)	K_D (10^{-3}mol^2/ kJ^2)	R^2
SPC(Cu-BTC)	223.71	0.0154	0.9943	8.7921	1.8752	0.8980	57.1364	0.2103	0.9769	128.1378	0.0144	0.7015
SPC(Zn-BTC)	289.12	0.0070	0.9853	8.4637	1.7213	0.9256	38.5023	0.1342	0.9737	165.6832	0.0249	0.6568
SPC(5-(C/Z-BTC))	458.11	0.0084	0.9921	12.6742	1.7289	0.9326	24.3652	0.1162	0.9825	256.3523	0.0362	0.6391

Table S6 Comparison of adsorption capacity of different adsorbents for PFOA.

Adsorbent	PFOA adsorption capacity (mg/g)	PFOA Adsorption equilibrium time (h)	References
MIL-101(Cr)	460	1	1
MIL-101(Cr)-NH_2	290	1	1
MIL-101(Cr)-NMe_2	493	1	1
MIL-101(Cr)-DMEN	534	1	1
MIL-101-Cr-QDMEN	754	1	1
ZIF-7	22	1	2
ZIF-8	177	2	2
ZIF-L	244	2	2
UiO-66	388	1	3
UiO-66-F4	467	1	3
UiO-67	743	1	3
MIL-125-NH_2	42	4	4
MIL-100-Fe	427	1.5	5
MIL-101-Fe	490	1.5	5
MIL-96-RHPAM2	340	186	6
NU-1000	507	0.5	7
PCN-999	1089	12	8
F-MOF	420	1/3	9
DUT-5-2	92	10	10
DFB-CDP	33	13	11
MWNTs	140	3	12
FCX4-P	189	2	13
AC	53	33.5	14
All-silica Beta (β)	371	6	15
CZDM-3	627	1	16
CMs	303	4	17
OMC-900	87	/	18
SPC(5-(C/Z-BTC))	460	2	This work

Table S7 Adsorption kinetic equations.

Name	Equations
Pseudo-first order model	$\ln(q_e - q_t) = \ln(q_{e,cal}) - K_1 t$
Pseudo-second order model	$\frac{t}{q_t} = \frac{1}{K_2 {q_e}^2} + \frac{t}{q_e}$
Intra-particle diffusion model	$q_t = K_3 t^{1/2}$
Dunwald-Wagnen diffusion model	$\ln(1 - E^2) = -kt$ $k = \frac{\pi^2}{{R_P}^2} D_{iq}$

where q_e and q_t (mg/g) are the sulfur uptake capacities at equilibrium and at time t (min), respectively, K_1 (1/min) is the adsorption rate constant, K_2 (g·mg^{-1}·min^{-1}) is the rate constant of the second-order equation, K_3 (mg·g^{-1}·min$^{-1/2}$) is the intra-particle diffusion rate constant.

Samples	Pseudo-first-order kinetic model						Pseudo-second-order kinetic model			Intra-particle diffusion model				
	$\ln(q_e-q_t)=\ln(q_{e\,cal})-K_1t$						$t/q_t=1/(K_2*q_e^2)+t/q_e$			$qt=K_3t^{0.5}+C$				
	$q_{e,exp}$ (mg/g)	$q_{e,cal}$ (mg/g)	K_1 (1/min)	R^2	$\triangle q$ (mg/g)	$\triangle q$ (%)	$q_{e,cal}$ (mg/g)	K_2 (g/mg▪min)	R^2	$\triangle q$ (mg/g)	$\triangle q$ (%)	C (mg/g)	K_3 (mg/g $Min^{1/2}$)	R^2
SPC(Cu-BTC)	210.35	85.61	0.0157	0.4938	124.74	59.30	233.62	0.0002	0.9681	23.27	11.06	40.67	13.11	0.7337
SPC(Zn-BTC)	291.57	217.02	0.0211	0.6726	74.55	25.57	353.4	0.0001	0.9419	61.83	21.21	15.05	20.86	0.8538
SPC(5-(C/Z-BTC))	427.39	722.51	0.0241	0.8409	295.12	59.15	534.83	0.0003	0.9256	107.44	25.14	53.79	33.95	0.9670

Table S8 Kinetics parameters on the adsorption of PFOA in solution by SPC(Cu-BTC) and others.

Table S9 Diffusion coefficients of PFOA adsorbed onto SPC(Cu-BTC), SPC(Zn-BTC) and SPC(5-(C/Z-BTC)).

Samples	K (min^{-1})	D_{iq} (*10^{-12} cm^2/s)
SPC(Cu-BTC)	0.008	0.018
SPC(Zn-BTC)	0.079	0.020
SPC(5-(Cu/Zn-BTC))	0.274	0.025

Table S10 Adsorption thermodynamic parameters equations.

Name	Equations
Gibbs equation	$\Delta G = -RT\ln K_d$
Van 't Hoff equation	$\ln K_d = -\frac{\Delta H}{RT} + \frac{\Delta S}{R}$

where ΔG ($KJ \cdot mol^{-1}$) is the change in Gibbs free energy for the adsorption reaction, ΔH ($KJ \cdot mol^{-1}$)is the change in enthalpy of adsorption, ΔS ($J \cdot mol^{-1} \cdot K^{-1}$) is the change in entropy of adsorption, K_d ($L \cdot mg^{-1}$) is the adsorption equilibrium constant, substituting the value of K_L ($L \cdot mg^{-1}$), R is the universal gas constant (8.314 $J \cdot mol^{-1} \cdot K^{-1}$), T is the temperature (K).

Sample	T (K)	ΔG (KJ·mol^{-1})	Ln(K)	ΔH (KJ·mol^{-1})	ΔS (J·mol^{-1}·K^{-1})
SPC(5-(Cu/Zn-BTC))	298.15	-0.032	0.01	-16.633	-55.060
	308.15	0.296	-0.12		
	318.15	0.603	-0.23		

Table S11 Thermodynamics adsorption parameters of PFOA onto SPC(5-(C/Z-BTC)).

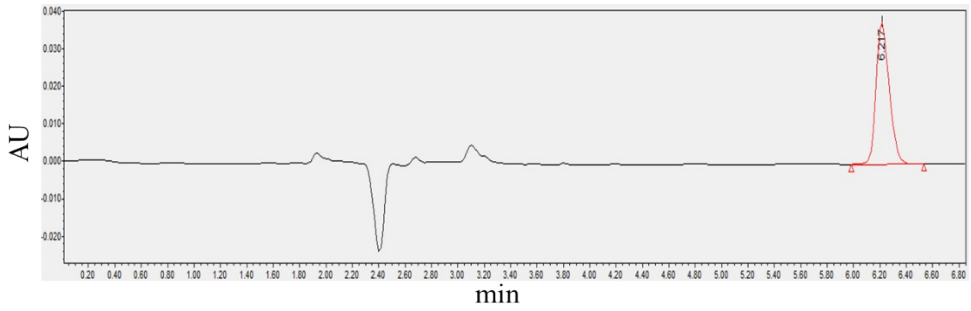

Fig. S1 The high-performance liquid chromatography chart of perfluorooctanoic acid.

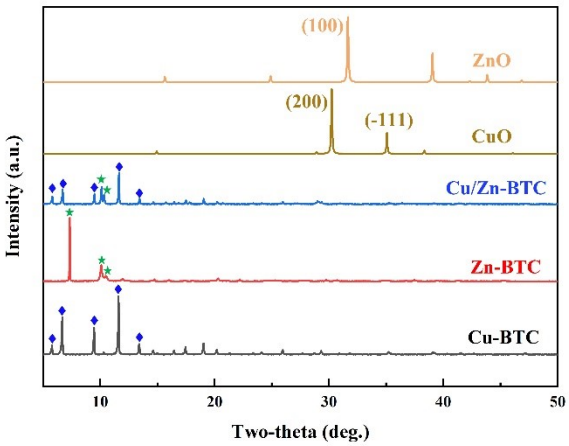

Fig. S2 XRD patterns and simulated curves.

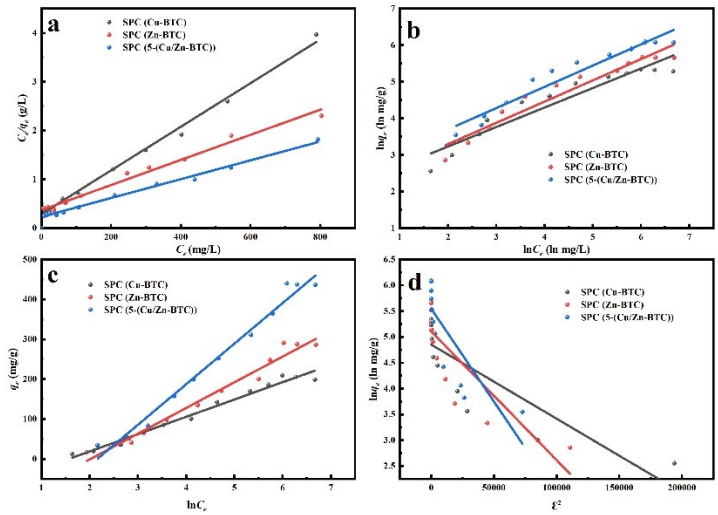

Fig. S3 The Langmuir (a), Freundlich (b), Temkin (c), and D-R (d) linear adsorption isotherm models of SPC(Cu-BTC), SPC(Zn-BTC), and SPC(5-(Cu/Zn-BTC)) for PFOA were established.

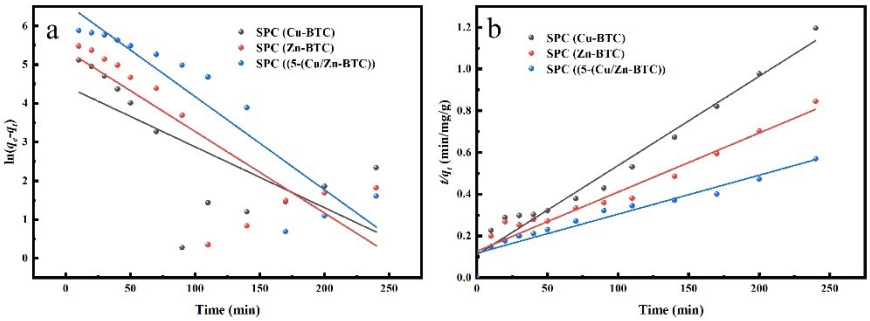

Fig. S4 The pseudo-first-order (a) and pseudo-second-order (b) kinetic models of PFOA adsorption on SPC(Cu-BTC), SPC(Zn-BTC), and SPC(5-(Cu/Zn-BTC)) were established.

REFERENCES

1 K. Liu, S. Zhang, X. Hu, K. Zhang, A. Roy and G. Yu, Understanding the adsorption of PFOA on MIL-101 (Cr)-based anionic-exchange metal–organic frameworks: comparing DFT calculations with aqueous sorption experiments, *Environ. Sci. Technol.*, 2015, **49**(14), 8657-8665.
2 M.-J. Chen, A.-C. Yang, N.-H. Wang, H.-C. Chiu, Y.-L. Li, D.-Y. Kang and S.-L. Lo, Influence of crystal topology and interior surface functionality of metal-organic frameworks on PFOA sorption performance, *Microporous Mesoporous Mater.*, 2016, **236**, 202-210.
3 K. Sini, D. Bourgeois, M. Idouhar, M. Carboni and D. Meyer, Metal–organic framework sorbents for the removal of perfluorinated compounds in an aqueous environment, *New J. Chem.*, 2018, **42**(22), 17889-17894.
4 R. Li, N.N. Adarsh, H. Lu and M. Wriedt, Metal-organic frameworks as platforms for the removal of per-and polyfluoroalkyl substances from contaminated waters, *Matter*, 2022, **5**(10), 3161-3193.
5 Y. Yang, Z. Zheng, W. Ji, J. Xu and X. Zhang, Insights to perfluorooctanoic acid adsorption micro-mechanism over Fe-based metal organic frameworks: Combining computational calculation with response surface methodology, *J. Hazard. Mater.*, 2020, **395**, 122686.
6 L.H.M. Azmi, D.R. Williams and B.P. Ladewig, Polymer-assisted modification of metal-organic framework MIL-96 (Al): influence of HPAM concentration on particle size, crystal morphology, and removal of harmful environmental pollutant PFOA, *Chemosphere*, 2021, **262**, 128072.
7 R. Li, S. Alomari, R. Stanton, M.C. Wasson, T. Islamoglu, O.K. Farha, T.M. Holsen, S.M. Thagard, D.J. Trivedi, M. Wriedt, Efficient removal of per-and polyfluoroalkyl substances from water with zirconium-based metal–organic frameworks, *Chem. Mater.*, 2021, **33**(9), 3276-3285.
8 R.-R. Liang, S. Xu, Z. Han, Y. Yang, K.-Y. Wang, Z. Huang, J. Rushlow, P. Cai, P. Samorì and H.-C. Zhou, Exceptionally high perfluorooctanoic acid uptake in water by a zirconium-based metal–organic framework through synergistic chemical and physical adsorption, *J. Am. Chem. Soc.*, 2024, **146**(14), 9811-9818.
9 S.-Y. Ma, J. Wang, L. Fan, H.-L. Duan and Z.-Q. Zhang, Preparation of a fluorinated metal-organic framework and its application for the dispersive solid-phase extraction of perfluorooctanoic acid, *J. Chromatogr. A*, 2020, **1611**, 460616.
10 Y. Hu, M. Guo, S. Zhang, W. Jiang, T. Xiu, S. Yang, M. Kang, Z. Dongye, Z. Li and L. Wang, Microwave synthesis of metal-organic frameworks absorbents (DUT-5-2) for the removal of PFOS and PFOA from aqueous solutions, *Micropor. Mesopor. Mater.*, 2022, **333**, 111740.
11 L. Xiao, Y. Ling, A. Alsbaiee, C. Li, D.E. Helbling and W.R. Dichtel, β-Cyclodextrin polymer network sequesters perfluorooctanoic acid at environmentally relevant concentrations, *J. Am. Chem. Soc.*, 2017, **139**(23), 7689-7692.
12 X. Li, H. Zhao, X. Quan, S. Chen, Y. Zhang and H. Yu, Adsorption of ionizable organic contaminants on multi-walled carbon nanotubes with different oxygen contents, *J. Hazard. Mater.*, 2011, **186**(1), 407-415.
13 D. Shetty, I. Jahovic, T. Skorjanc, T.S. Erkal, L. Ali, J. Raya, Z. Asfari, M.A. Olson, S. Kirmizialtin and A.O. Yazaydin, Rapid and efficient removal of perfluorooctanoic acid from water with fluorine-rich calixarene-based porous polymers, *ACS Appl. Mater. Interfaces*, 2020, **12**(38), 43160-43166.
14 D. Zhang, Q. Luo, B. Gao, S.-Y.D. Chiang, D. Woodward and Q. Huang, Sorption of perfluorooctanoic acid, perfluorooctane sulfonate and perfluoroheptanoic acid on granular activated carbon, *Chemosphere*, 2016, **144**, 2336-2342.
15 M. Van den Bergh, A. Krajnc, S. Voorspoels, S.R. Tavares, S. Mullens, I. Beurroies, G. Maurin,

G. Mali and D.E. De Vos, Highly selective removal of perfluorinated contaminants by adsorption on all-silica zeolite beta, *Angew. Chem.*, 2020, **132**(33), 14190-14194.

16 H. Lin, Z. Xia, K. Xue, X. Zhou, Y. Yao, N. Ma and W. Dai, Synergistically enhanced capture of perfluorooctanoic acid using a novel dual metal-organic framework adsorbent, *Particuology*, 2025, **132**(33), 130-142.

17 A. Sánchez-Yepes, A.P. Ferreira, A. Santos, A. Romero, H.T. Gomes and D. Lorenzo, Novel Carbon-Based Materials for Sustainable Water Treatment: Perfluorooctanoic Acid Adsorption and Adsorbent Regeneration via Thermally Activated Persulfate Oxidation, *J. Environ. Chem. Eng.*, 2025, 120084.

18 X. Lei, L. Yao, Q. Lian, X. Zhang, T. Wang, W. Holmes, G. Ding, D.D. Gang and M.E. Zappi, Enhanced adsorption of perfluorooctanoate (PFOA) onto low oxygen content ordered mesoporous carbon (OMC): Adsorption behaviors and mechanisms, *J. Hazard. Mater.*, 2022, **421**, 126810.